University of Zurich[UZH]

Zurich Open Repository and Archive
University of Zurich
Main Library
Strickhofstrasse 39
CH-8057 Zurich
www.zora.uzh.ch

Year: 2008

Clumps and streams in the local dark matter distribution

Diemand, J ; Kuhlen, M ; Madau, P ; Zemp, M ; Moore, B ; Potter, D ; Stadel, J

Abstract: In cold dark matter cosmological models1,2, structures form and grow through the merging of smaller units3. Numerical simulations have shown that such merging is incomplete; the inner cores of haloes survive and orbit as 'subhaloes' within their hosts4,5. Here we report a simulation that resolves such substructure even in the very inner regions of the Galactic halo. We find hundreds of very concentrated dark matter clumps surviving near the solar circle, as well as numerous cold streams. The simulation also reveals the fractal nature of dark matter clustering: isolated haloes and subhaloes contain the same relative amount of substructure and both have cusped inner density profiles. The inner mass and phasespace densities of subhaloes match those of recently discovered faint, dark-matter-dominated dwarf satellite galaxies6–8, and the overall amount of substructure can explain the anomalous flux ratios seen in strong gravitational lenses9,10. Subhaloes boost c-ray production from dark matter annihilation by factors of 4 to 15 relative to smooth galactic models. Local cosmic ray production is also enhanced, typically by a factor of 1.4 but by a factor of more than 10 in one per cent of locations lying sufficiently close to a large subhalo. (These estimates assume that the gravitational effects of baryons on dark matter substructure are small.)

DOI: https://doi.org/10.1038/nature07153

Posted at the Zurich Open Repository and Archive, University of Zurich
ZORA URL: https://doi.org/10.5167/uzh-16552
Journal Article

Originally published at:
Diemand, J; Kuhlen, M; Madau, P; Zemp, M; Moore, B; Potter, D; Stadel, J (2008). Clumps and streams in the local dark matter distribution. Nature, 454(7205):735-738.
DOI: https://doi.org/10.1038/nature07153

arXiv:0805.1244v1 [astro-ph] 8 May 2008

Clumps and streams in the local dark matter distribution

J. Diemand[1], M. Kuhlen[2], P. Madau[1], M. Zemp[1], B. Moore[3], D. Potter[3], & J. Stadel[3]

[1]*University of California, Department of Astronomy and Astrophysics, Santa Cruz, CA 95064, USA.*

[2]*Institute for Advanced Study, Einstein Drive, Princeton, NJ 08540, USA.*

[3]*University Zurich, Institute for Theoretical Physics, Winterthurerstrasse 190, 8057 Zurich, Switzerland.*

In the standard "cold dark matter" cosmological model[1,2] structures form and grow by merging of smaller subunits[3]. Cosmological simulations have demonstrated that most mergers are incomplete: many halos survive and orbit as "subhalos" within their hosts[4,5]. So far, subhalos have not been resolved in the very inner halo and it was unclear whether the local dark matter would be smooth or clumpy. We have simulated the formation of the Galactic halo at an unprecedented resolution that allows us for the first time to resolve local substructure. We find hundreds of very concentrated dark matter clumps surviving near the solar system, as well as numerous cold streams. These small, dark Galactic ghost halos are survivers of the merging hierarchy and have properties remarkably close to their isolated counterparts in the field: both have cuspy inner density profiles and both contain the same relative amount of substructure. These predictions have various implications: Dark matter annihilation rates would be significantly enhanced. They match the inner densities[6] and phase-space densities[7] of the recently discovered faint, dark matter-dominated dwarf satellites[8] and they compare well with substructure constraints from gravitational lensing[9,10].

The theoretical framework for the evolution of a cold dark matter (CDM) dominated

Universe was established 25 years ago[1,2]. The growth of cosmic structures begins early in this model on Earth mass scale[11,12], and continues from the bottom up until galaxy clusters form that are twenty orders of magnitude more massive. Galaxies are embedded within extended halos of dark matter, which form through the gravitationally-induced aggregation of many smaller progenitors[3]. There is about five times less ordinary baryonic matter than dark matter so the dynamics are usually dictated by the dark matter. Baryons dominate only in the centers of large halos, where galaxies form. Our calculations neglect the effects of baryons, which is a good approximation for the small halos we focus on here, since most of them remain completely dark and a few of them will host a dark matter dominated dwarf galaxy.

The CDM model has been remarkably successful at describing the large-scale mass distribution of our Universe from the hot Big Bang to the present. The nature of the dark matter particle is best tested, however, on small scales where its interaction properties manifest themselves by modifying the structure of galaxy halos and their substructure. Resolving small-scale CDM structures is extremely challenging, as the range of lengths, masses, and timescales that need to be simulated is immense. Here we present the most accurate predictions about small scale clustering and the first constraints on the local subhalo abundance and properties. They are based on the highest precision calculation – dubbed "Via Lactea II" – of the assembly of the Galactic CDM halo. The simulation follows the growth of a Milky Way-size halo in a ΛCDM Universe from redshift 100 to the present. It used over a million processor hours on the "Jaguar" Cray XT3 supercomputer at the Oak Ridge National Laboratory. We used the parallel treecode PKDGRAV2[13] and sample the galaxy-forming region with 1.1×10^9 particles of mass $4,100\,M_\odot$. Cosmological parameters were taken from *WMAP*[14].

The wealth of substructure that survives the hierarchical assembly process to the present epoch is clearly seen in Figure 1: we resolve over 40,000 subhalos within 400 kpc of the center and they are distributed approximately with equal mass per decade

of mass over the range $10^6 - 10^9\,M_\odot$. They have very large inner phase-space densities ($\gtrsim 10^{-5}\,\mathrm{M_\odot\,pc^{-3}\,km^{-3}\,s^3}$) due to their steep inner density cusps and their relatively small internal velocity dispersions. This agrees well with the extremely high stellar phase-space densities observed recently in ultra faint dwarf galaxies[7]. Our predicted inner subhalo densities ($0.4 - 2.5\,M_\odot$ pc^{-3} within 100 pc, $7 - 46\,M_\odot$ pc^{-3} within 10 pc) are also perfectly consistent with the observations[6,7]. The fact that CDM naturally predicts a small-scale dark matter distribution that matches the observations is a real success of the model. Particle candidates that introduce a phase-space limit, such as a sterile neutrino, or have a high collisional cross section such as self interacting dark matter would fail these fundamental observational tests.

The phase-space map (upper inset in Figure 1) also contains coherent elongated features. These are streams which form out of material removed from accreted and disrupted subhalos. The few visible streams have quite low densities (about 100 times below the local density) but owing to their low velocity dispersion (about 10 times smaller than that of background particles) they just barely manage to stand out in local phase space density (these streams have about $10^{-9}\,\mathrm{M_\odot\,pc^{-3}\,km^{-3}\,s^3}$). In cases where the disrupted subhalo hosted a luminous satellite galaxy, the resulting streams would contain not only dark matter but also stars. This process would then produce detectable features in the Milky Way's stellar halo, like those observed in the "Field of Streams"[15].

Further evidence for halo substructure comes from the anomalous flux ratios in multiply-imaged gravitationally lensed quasars[16,17]. Perturbations to the light path from substructure can explain this phenomenon if the projected substructure fraction within 10 kpc is about one percent[9,10]. Within a projected distance of 10 kpc from the center, 0.50% of the host mass belongs to resolved substructure, which could be just enough to explain the observed flux anomalies. In earlier simulations this fraction was lower, even the first Via Lactea halo[18] had only 0.23%. The improved mass and time resolution of Via Lactea II allows to resolve more of the inner substructure (Figure 3). Somewhat smaller subhalos than those

resolved here might also contribute to the observed anomalies. Extrapolating the subhalo mass function from $10^6\,M_\odot$ down to $10^3\,M_\odot$ increases the projected substructure fraction to one percent.

Via Lactea II predicts a remarkable self-similar pattern of clustering properties: We find that both host and subhalos have the same cuspy inner density profiles and the same relative abundances of substructure. This simulation is the first to use extremely accurate integration of the particle orbits in high density regions[19], allowing for the first time an accurate determination of the density profile within the inner kpc of the Galactic halo and within the centers of its satellite galaxies. We find that a cuspy profile fits the host halos density profile well, while the best fit cored profile lies below the simulated inner densities (Figure 2). The inner profiles of subhalos are also consistent with cusps over their resolved ranges. They scatter around the moderate cusp index of the host halo ($\gamma = 1.24$): Some of them are denser in the inner part, and some are less dense, exactly like the inner parts of *field* halos, which have inner slopes of $\gamma \simeq 1.2 \pm 0.2$[20]. At large radii subhalo density profiles generally fall off faster than field halo profiles. These similarities and differences between subhalo and field halo profiles have a simple explanation: Subhalo density profiles were modified by tidal mass loss, which removes material from the outside in, but does not change the inner cusp structure[18,21]. Figure 3 shows that the dwarf satellites of the Milky Way appear to be scaled versions of the main halo not just in their inner mass distribution, but also in term of relative substructure abundances. Via Lactea II demonstrates the fractal-like appearance of the dark matter by resolving the second generation of surviving sub-substructures from the merging hierarchy. This suggest that at infinite resolution one would find a long nested series of halos within halos within halos etc., reminiscent of a Russian Matryoshka doll, all the way down the first and smallest halos.

The multitude of dark substructures increases the dark matter annihilation signal, since it is proportional to the *square* of the local density. For cuspy profiles (Figure 2) with some

fixed inner slope ($\gamma < 1.5$) one gets the following simple scaling relation for the annihilation:

$$L \propto \rho_s^2 r_s^3 \propto V_{\rm max}^4 / r_{\rm Vmax} \propto V_{\rm max}^3 \sqrt{c_V} \ , \tag{1}$$

see Figure 4 for the definition of the concentration c_V and its values. Combined with the steep subhalo velocity function $N(> V_{\rm max}) \propto V_{\rm max}^{-3}$, this implies that subhalos of all sizes contribute about equally to the total signal of a halo. Taking the higher concentrations of smaller systems[22] into account, one finds that small subhalos are contributing more than large ones[23,24]. Summing up $V_{\rm max}^4/r_{\rm Vmax}$ of all resolved subhalos in Via Lactea II comes close (97%) to the host halo's $V_{\rm max}^4/r_{\rm Vmax}$, i.e. the resolved subhalos already contribute as much as their smooth host alone would. In other words the "substructure boost factor" is at least 1.97. Extrapolating down to micro-subhalos of size $V_{\rm max} = 0.25\,{\rm m\,s^{-1}}$, taking into account how concentrations depend on subhalo size[22] and position (Figure 4), and assuming a uniform distribution of subhalo inner slopes α between 1.0 and 1.5, leads to a total boost of 14.6. Most of it comes from very small clumps: halting the same extrapolation at $V_{\rm max} = 44\,{\rm m\,s^{-1}}$ lowers the boost to 6.6, and stopping at $V_{\rm max} = 2\,{\rm km\,s^{-1}}$ yields a factor of only 2.7. While the contribution from small, dark clumps itself is not affected by baryons, it may not dominate the total signal in scenarios in which baryonic collapse greatly increases the central dark matter densities in larger halos. However, the net effect of stars, black holes, and galaxy formation is unclear, and it may actually lead to a reduction in the central dark matter densities. The detailed distribution of cusp indices is still unknown, since only a few halos have been simulated with sufficient resolution[20]. For the annihilation boost factors the existence of a few steep cusps near 1.5 would make a big difference, since the signal diverges logarithmically towards the center in a $\gamma = 1.5$ cusp. Cutting the assumed uniform distribution of inner slopes at 1.4 instead of 1.5 gives a boost of 9.9 instead of 14.6. These factors imply that most of the extra-galactic γ-ray background from dark matter annihilation[23], which will be constrained or even detected by the upcoming GLAST mission, should be emitted by subhalos, and not by distinct host halos.

Besides γ-rays, dark matter annihilation would produce charged particles and anti-

particles, which propagate over much smaller distances within the Galaxy. Space based experiments (like PAMELA, and in the near future AMS-02) could detect anti-particles produced in dark matter annihilations within about one kiloparsec[25]. What fraction of this local annihilation would happen in nearby subhalos? To constrain this local boost factor we use the same assumptions as above ($\gamma = [1 - 1.5]$,$V_{\rm max} \geq 0.25\,{\rm m\,s^{-1}}$), but now we only include subhalos within one kiloparsec of the solar system (see Figure 4 for the local subhalo abundance). The resulting signal is 40% of the smooth halo signal, which we estimated using the spherically averaged density at 8 kpc ($\rho_0 = 0.40$ GeV c^{-2} cm^{-3}). In other words, the typical local boost factor is 1.4. Explaining the positron excess from the HEAT experiment[26] with local dark matter annihilation requires enhancements from about 3 to 100[25]. When a relatively large subhalo happens to lie within 1 kpc, one can get the higher boost factors without violating the local subhalo constraints from our simulation. Such cases are possible, but not likely: Only 5.2 percent of all random realizations have a boost factor of 3 or larger (caused by a $V_{\rm max} \geq 3.4\,{\rm km\,s^{-1}}$ clump within 1 kpc). In 1.0 percent of the cases the boost factor reaches 10 or higher due to a nearby, large $V_{\rm max} \geq 5.6\,{\rm km\,s^{-1}}$ subhalo.

We have pushed supercomputing technology to its limits in order to calculate the small-scale structure of our Galactic halo - confirming these predictions is the ultimate test of the standard cosmological model and is well within reach of forthcoming observations and experiments. Large data sets of halo star radial velocities (e.g. from *SEGUE*, the Sloan Extension for Galactic Understanding and Exploration, and *RAVE*, the RAdial Velocity Experiment) and ultimately proper motions (from ESA's astrometry space mission *GAIA*) together with detailed dynamical stellar halo models based on cosmological simulations like Via Lactea II will make it possible to determine the mass distribution and formation history of the Milky Way in detail.

1. Peebles, P. J. E. Large-scale background temperature and mass fluctuations due to scale-invariant primeval perturbations. *ApJL* **263**, L1–L5 (1982).

2. Blumenthal, G. R., Faber, S. M., Primack, J. R. & Rees, M. J. Formation of galaxies

and large-scale structure with cold dark matter. *Nature* **311**, 517–525 (1984).

3. White, S. D. M. & Rees, M. J. Core condensation in heavy halos - A two-stage theory for galaxy formation and clustering. *MNRAS* **183**, 341–358 (1978).

4. Ghigna, S. *et al.* Dark matter haloes within clusters. *MNRAS* **300**, 146–162 (1998).

5. Klypin, A., Kravtsov, A. V., Valenzuela, O. & Prada, F. Where Are the Missing Galactic Satellites? *ApJ* **522**, 82–92 (1999).

6. Strigari, L. E. *et al.* The Most Dark Matter Dominated Galaxies: Predicted Gamma-ray Signals from the Faintest Milky Way Dwarfs. *ArXiv e-prints* (2007). `0709.1510`.

7. Simon, J. D. & Geha, M. The Kinematics of the Ultra-faint Milky Way Satellites: Solving the Missing Satellite Problem. *ApJ* **670**, 313–331 (2007).

8. Belokurov, V. *et al.* Cats and Dogs, Hair and a Hero: A Quintet of New Milky Way Companions. *ApJ* **654**, 897–906 (2007).

9. Dalal, N. & Kochanek, C. S. Direct Detection of Cold Dark Matter Substructure. *ApJ* **572**, 25–33 (2002).

10. Metcalf, R. B., Moustakas, L. A., Bunker, A. J. & Parry, I. R. Spectroscopic Gravitational Lensing and Limits on the Dark Matter Substructure in Q2237+0305. *ApJ* **607**, 43–59 (2004).

11. Green, A. M., Hofmann, S. & Schwarz, D. J. The power spectrum of SUSY-CDM on subgalactic scales. *MNRAS* **353**, L23–L27 (2004).

12. Diemand, J., Moore, B. & Stadel, J. Earth-mass dark-matter haloes as the first structures in the early Universe. *Nature* **433**, 389–391 (2005).

13. Stadel, J. G. Cosmological N-body simulations and their analysis. *PhD Thesis, University of Washington* (2001).

14. Spergel, D. N. *et al.* Three-Year Wilkinson Microwave Anisotropy Probe (WMAP) Observations: Implications for Cosmology. *ApJS* **170**, 377–408 (2007).

15. Belokurov, V. *et al.* The Field of Streams: Sagittarius and Its Siblings. *ApJL* **642**, L137–L140 (2006).

16. Mao, S. & Schneider, P. Evidence for substructure in lens galaxies? *MNRAS* **295**, 587–+ (1998).

17. Metcalf, R. B. & Madau, P. Compound Gravitational Lensing as a Probe of Dark Matter Substructure within Galaxy Halos. *ApJ* **563**, 9–20 (2001).

18. Diemand, J., Kuhlen, M. & Madau, P. Formation and Evolution of Galaxy Dark Matter Halos and Their Substructure. *ApJ* **667**, 859–877 (2007).

19. Zemp, M., Stadel, J., Moore, B. & Carollo, C. M. An optimum time-stepping scheme for N-body simulations. *MNRAS* **376**, 273–286 (2007).

20. Diemand, J., Moore, B. & Stadel, J. Convergence and scatter of cluster density profiles. *MNRAS* **353**, 624–632 (2004).

21. Kazantzidis, S. *et al.* Density Profiles of Cold Dark Matter Substructure: Implications for the Missing-Satellites Problem. *ApJ* **608**, 663–679 (2004).

22. Bullock, J. S. *et al.* Profiles of dark haloes: evolution, scatter and environment. *MNRAS* **321**, 559–575 (2001).

23. Ullio, P., Bergström, L., Edsjö, J. & Lacey, C. Cosmological dark matter annihilations into γ rays: A closer look. *Phys. Rev. D* **66**, 123502–+ (2002).

24. Colafrancesco, S., Profumo, S. & Ullio, P. Multi-frequency analysis of neutralino dark matter annihilations in the Coma cluster. *A&A* **455**, 21–43 (2006). arXiv:astro-ph/0507575.

25. Lavalle, J., Yuan, Q., Maurin, D. & Bi, X. . Full Calculation of Clumpiness Boost factors for Antimatter Cosmic Rays in the light of \LambdaCDM N-body simulation results. *ArXiv e-prints* **709** (2007).

26. Beatty, J. J. *et al.* New Measurement of the Cosmic-Ray Positron Fraction from 5 to 15GeV. *Physical Review Letters* **93**, 241102–+ (2004).

27. Sharma, S. & Steinmetz, M. Multidimensional density estimation and phase-space structure of dark matter haloes. *MNRAS* **373**, 1293–1307 (2006).

28. Bertschinger, E. Multiscale Gaussian Random Fields and Their Application to Cosmological Simulations. *ApJS* **137**, 1–20 (2001).

29. Navarro, J. F. *et al.* The inner structure of ΛCDM haloes - III. Universality and asymptotic slopes. *MNRAS* **349**, 1039–1051 (2004).

30. Reed, D. *et al.* Dark matter subhaloes in numerical simulations. *MNRAS* **359**, 1537–1548 (2005).

Acknowledgements It is a pleasure to thank Bronson Messer and the Scientific Computing Group at the National Center for Computational Sciences for their help. The "Via Lactea II" simulation was performed at the Oak Ridge National Laboratory through an award from DOE's Office of Science as part of the 2007 Innovative and Novel Computational Impact on Theory and Experiment (INCITE) program. Additional computations (initial conditions generation and code optimisations) were carried out on the MareNostrum supercomputer at the BSC and on Columbia at NASA Ames. This work was supported by NASA and the Swiss National Science Foundation.

Competing Interests The authors declare that they have no competing financial interests.

Correspondence Correspondence and requests for materials should be addressed to J. D. (email: diemand@ucolick.org).

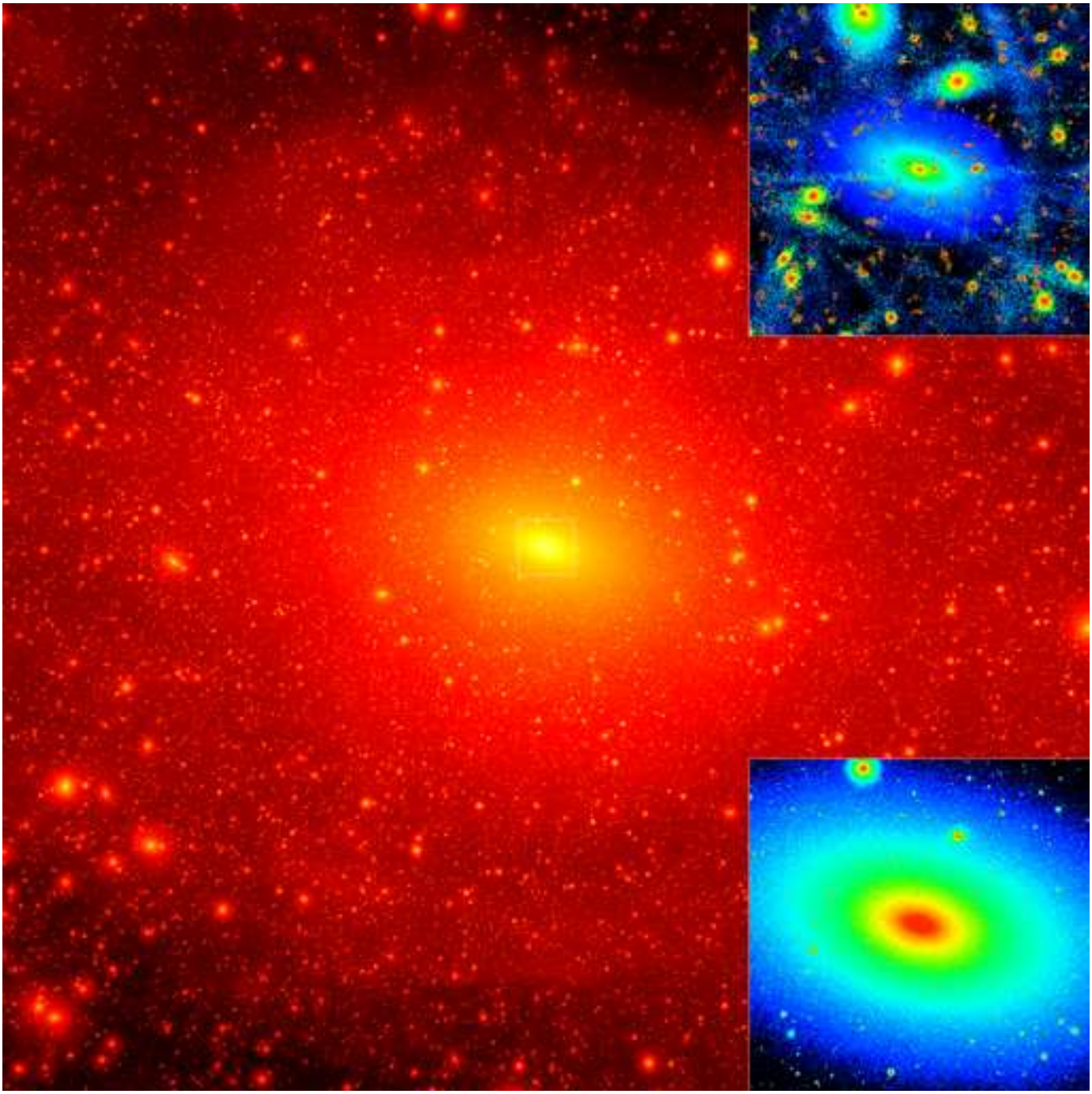

Figure 1: Projected dark matter density-square map of "Via Lactea II". An 800 kpc cube is shown. The insets focus on an inner 40 kpc cube, in local density (bottom), and in local phase space density calculated with EnBiD[27] (top). The Via Lactea II simulation has a mass resolution of 4,100 $M_\odot$ and a force resolution of 40 pc. It uses a new method to assign physical, adaptive time-steps[19] equal to 1/16 of the local dynamical timescale (but not shorter than 268,000 yr). This time-stepping allows to resolve high densities and it is the main improvement over Via Lactea I, which had 5 times heavier particles and force resolution of 90 pc. The enclosed densities within 300 pc of large subhalos are about twice as high in Via Lactea II, which allows them to survive closer to the Galaxy center. Initial conditions were generated with a modified, parallel version of GRAFIC2[28]. The high resolution region is embedded within a large periodic box (40 comoving Mpc) to account for the large scale tidal forces. The mass within 402 kpc (the radius enclosing 200 times the mean matter density) is $1.9 \times 10^{12}\, M_\odot$.

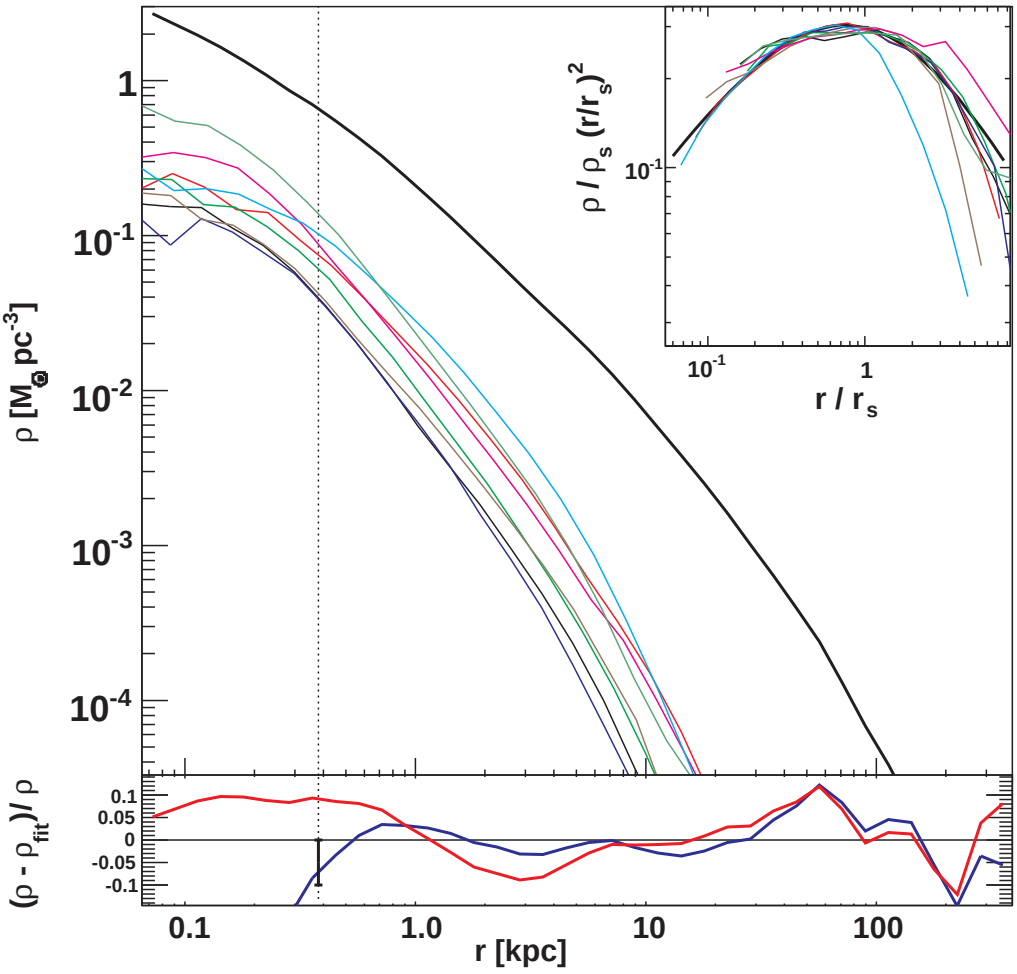

Figure 2: Density profiles of main halo and subhalos. *Main panel*: Profile of the Milky Way halo (*thick line*) and of eight large subhalos (*thin lines*). The *lower panel* gives the relative differences between the simulated main halo profile and a fitting formula with a core[29] $\rho(r) = \rho_s \exp\{-2/\alpha\,[(r/r_s)^\alpha - 1]$, with best fit parameters: $\alpha = 0.170$, $r_s = 21.5\,\mathrm{kpc}$, $\rho_s = 1.73 \times 10^{-3}\,\mathrm{M_\odot\,pc^{-3}}$ (*red curve*) and one with a cusp[20] $\rho(r) = \rho_s (r/r_s)^{-\gamma}(r/r_s + 1)^{-3+\gamma}$ with a best fit inner slope of $\gamma = 1.24$, $r_s = 28.1\,\mathrm{kpc}$, $\rho_s = 3.50 \times 10^{-3}\,\mathrm{M_\odot\,pc^{-3}}$ (*blue curve*). The vertical dotted line indicates the estimated convergence radius of 380 pc: simulated local densities are only lower limits inside of 380 pc and they should be correct to within 10% outside this region. The cuspy profile is a good fit to the inner halo, while the cored profile has a too shallow slope in the inner few kpc, causing it to overestimate densities around 4 kpc and to underestimate them at all radii smaller than 1 kpc. The simulated densities are higher than the best fit cored profile even at 80 pc, where they are certainly underestimated due to numerical limitations. We find the same behavior in the inner few kpc in all six snapshots we have analyzed so far between z=3 an z=0. The large residuals in the outer halos on the other hand are transient features, they are different in every snapshot. *Inset*: Rescaled host (thick line) and subhalo (thin lines) density profiles multiplied by radius square to reduce the vertical range of the figure.

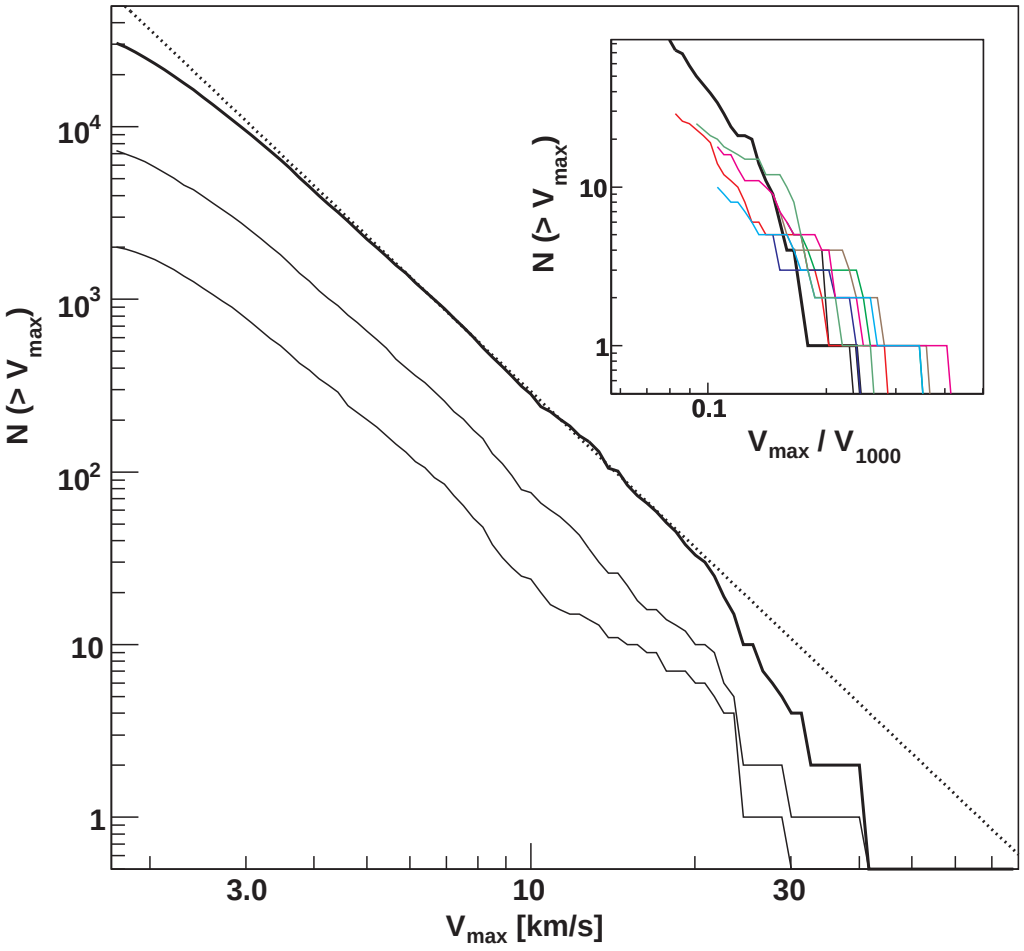

Figure 3: Subhalo and sub-subhalo abundances. Number of subhalos above $V_{\rm max}$ within $r_{200} = 402$ kpc (thick solid lines) and within 100 and 50 kpc of the galactic center (thin solid lines). $V_{\rm max}$ is the peak height of the subhalo circular velocity $v_{circ} = \sqrt{GM(<r)/r}$ and serves as a simple proxy for the mass of a subhalo. The dotted line is $N(>V_{\rm max}) = 0.036\,(V_{\rm max}/V_{\rm max,host})^{-3}$, where $V_{\rm max,host} = 201\,{\rm km\,s^{-1}}$ (at $r_{\rm Vmax,host} = 60$ kpc). It fits the subhalo abundance above $V_{\rm max} \simeq 3.5\,{\rm km\,s^{-1}}$. The number of smaller subhalos is artificially reduced by numerical limitations. Inside r_{200} this halo has 1.7 times more substructure than the first Via Lactea halo[18], a factor well within the halo-to-halo scatter[30]. Inside 50 kpc the difference grows to 2.6, probably due to the improved mass and time resolution of Via Lactea II, which allows to resolve inner substructure better. The *inset* shows the sub-subhalo abundance within r_{1000} (enclosing 1000 times the mean matter density) of the centers of eight (same ones as in Fig. 2) large subhalos (thin solid lines). r_{1000} is well inside of the tidal radius for these systems. The thick solid line shows the subhalo abundace of the host halo inside of its $r_{1000} = 213$ kpc. The (sub-)subhalo $V_{\rm max}$ values are given in units of $V_{1000} = \sqrt{GM(<r_{1000})/r_{1000}}$ of the corresponding host (sub-)halo. Lines stop at $V_{\rm max} = 2\,{\rm km\,s^{-1}}$. The mean sub-substructure abundance is consistent with the scaled down version of main halo, and both the mean abundance and the scatter agree with results in[30] for distinct *field* halos.

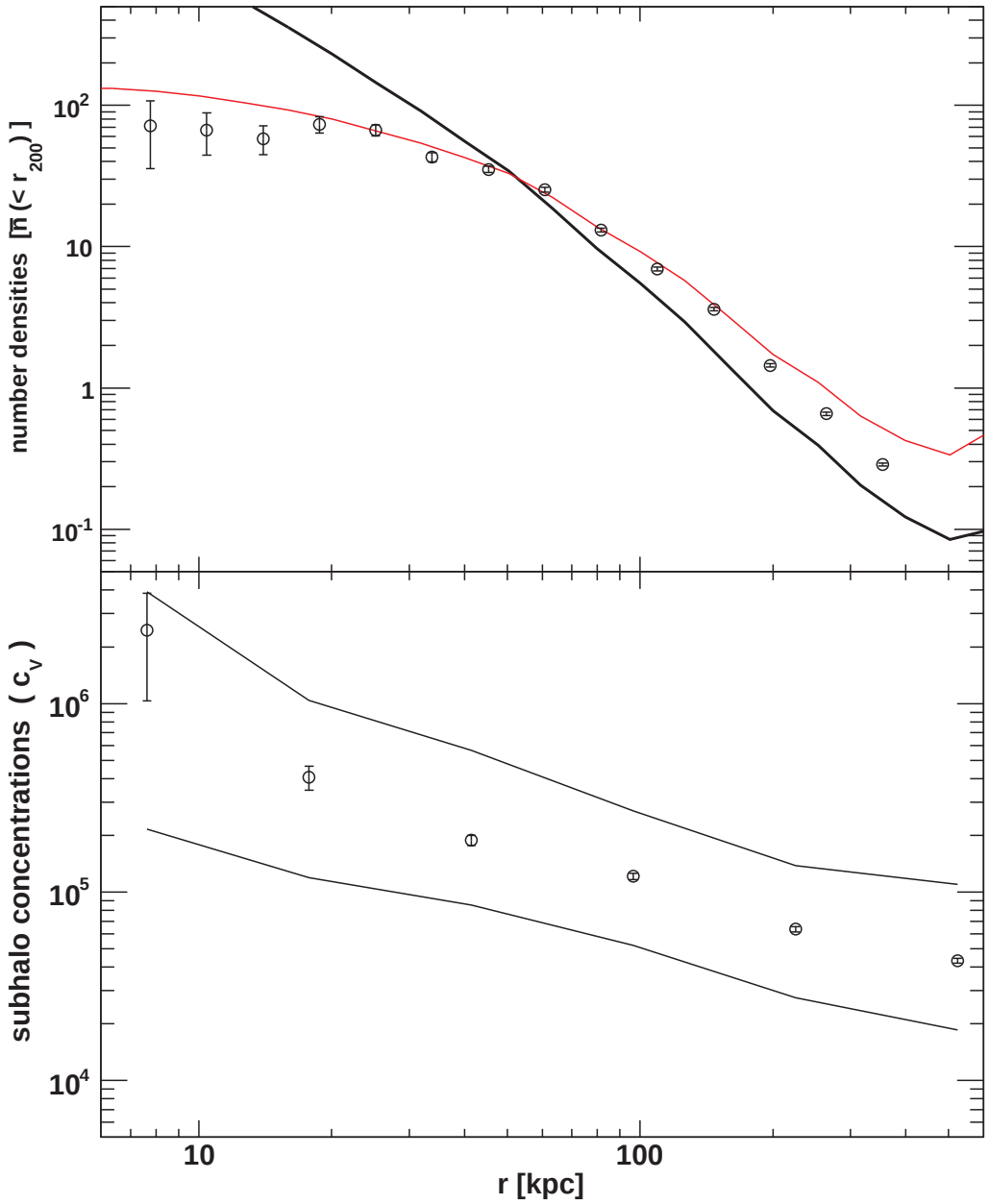

Figure 4: Abundance and concentrations of subhalos vs. distance from the galactic center. *Top:* The number density profile of subhalos (circles) is more extended than the dark matter density profile $\rho(r)$ (thick line). Their ratio turns out to be roughly proportional to the enclosed mass $M(<r)$, i.e. $\rho M(<r)$ (thin line) matches the subhalo number density quite well. Only subhalos larger than $V_{\rm max} = 3\,{\rm km\,s^{-1}}$ are included here. We find that the radial distribution does not depend on subhalo size. *Bottom:* Subhalo concentrations (median and 68% range are shown) increase towards the center, where the stronger tidal force remove more of the outer, low density parts from the subhalos. Subhalo concentrations are defined as the mean density within $r_{\rm Vmax}$, the radius of peak circular velocity[18]: $c_V \equiv \bar{\rho}(<r_{\rm Vmax})/\rho_{\rm crit,0} = (V_{\rm max}/r_{\rm Vmax})^2\, 4\pi/(3G\rho_{\rm crit,0})$, where $\rho_{\rm crit,0} \simeq 1.48\times10^{-7}\,{\rm M_\odot\,pc^{-3}}$. To make sure their c_V are resolved, only subhalos larger than $V_{\rm max} = 5\,{\rm km\,s^{-1}}$ are used. The error bars indicate the statistical uncertainties in both panels.